Shielding of the electromagnetic field of a coplanar waveguide by a metal film

Matthieu Bailleul

Shielding of the electromagnetic field of a coplanar waveguide by a metal film

Matthieu Bailleul*

Institut de Physique et Chimie des Matériaux de Strasbourg,

UMR 7504 CNRS-Université de Strasbourg, 67034 Strasbourg, France.

(Dated: July 1, 2013)

Abstract

In this letter, we show that the propagation of microwave fields along a planar transmission line is strongly modified when a conducting film is brought close to it. The effect is attributed to the shielding of the electrical and/or magnetic microwave fields which is shown to occur over a wide range of parameters (microwave frequency, film square resistance, transverse dimensions of the waveguide). This is illustrated by finite-element electromagnetic simulations and interpreted using a distributed impedance model. We discuss the implications of this phenomenon for broadband measurements of ferromagnetic resonance realized by placing a ferromagnetic metal film above a coplanar waveguide.

Most spintronics devices rely on thin ferromagnetic metal films (Fe, Co, Ni and their alloys). Because these devices are often to be operated in the high frequency (GHz) regime, in which the phenomenon of ferromagnetic resonance (FMR) occurs, it is essential to characterize precisely their microwave magnetic response. For this purpose, broadband techniques using transmission lines have been developed in the last fifteen years. In such techniques, a portion of the ferromagnetic film is placed close to the surface of a planar transmission line, in most cases a coplanar waveguide (CPW). The microwave magnetic field **H** delivered by the CPW excites the precession of the magnetization of the film which, in turn, induces an additional microwave voltage on the CPW. In practice, the FMR signal is extracted from the reflection-transmission coefficients of the loaded transmission line, measured as a function of the external magnetic field and the microwave frequency. The technique is referred to as Coplanar Waveguide FerroMagnetic Resonance (CPW-FMR),[1,2] Network-Analyzer FMR,[3–5] broad-band FMR,[6] or Pulse-Induced Microwave Magnetometer (PIMM)[7] in its time-domain implementation. Although the technique is relatively straightforward to implement, the extraction of the magnetic parameters from the measured microwave response requires some precautions. In particular, proper de-embedding techniques should be used to treat the propagation of the microwaves along the CPW,[3] and the transverse inhomogeneity of the microwave magnetic field should be accounted for in the interpretation of the FMR frequencies and linewidth.[8] Another very important point was recognized only very recently: the films to be measured are usually strongly conducting [typically 30 Ω/square for a 10 nm thick permalloy ($Py = Ni_{80}Fe_{20}$) film], which results in a strong modification of the distribution of the electric and magnetic microwave fields close to the film. This was described by Kostylev in terms of a shielding of the microwave field by eddy currents flowing along the conducting film:[9] calculations in simplified plane wave propagation geometries indicate that this effect occurs for a wide range of film thicknesses, even much below typical microwave skin depth which is of the order of several hundreds of nanometers for the materials usually investigated by CPW-FMR. Moreover, it has been shown that the eddy currents are responsible for the excitation of FMR modes having a non-uniform distribution of the oscillating magnetization across the film thickness[6,10] (so-called perpendicular standing spin wave modes) which could not be excited in the absence of shielding.

In this letter, we build upon these previous works by addressing the phenomenon of shielding in a realistic coplanar waveguide geometry with the help of finite element elec-

tromagnetic simulations. Then a simple interpretation is given within the conventional formalism of transmission lines. Finally we compare the observed phenomenon to the effect of slow-wave propagation well-known in the community of microwave engineering and discuss how the phenomenon of shielding could be accounted for in further developments of broadband FMR techniques.

The geometry used for the simulation is shown in Fig. 1(a). It consists of a conventional coplanar waveguide (a $t = 50$ μm thick $w = 350$ μm wide track surrounded by two lateral ground planes with gaps $g = 170$ μm) complemented with an additional ground plane and two vertical walls enclosing a $e = 200$ μm thick substrate of relative permittivity $\epsilon_r = 3.55$. This geometry, known as a channelized coplanar waveguide (CCPW) has the advantage of allowing single mode operation up to relatively high frequencies, due to the full metallization around the substrate providing a high cut-off frequencies for parasitic non-TEM modes.[11] The design of Fig. 1(a) mimics the transverse cross-section of test boards fabricated using conventional printed circuit board techniques over a RO4003 substrate (Rogers Corp.) which demonstrates single mode operation up to 50 GHz.[11] The space above the CPW is enclosed in an air box of thickness $h_{air} = 340$ μm. All the metallic boundaries defining the CCPW are assumed to be perfectly conducting. A metal film of square resistance R_{sq} is located above the CPW at a height $h = 30$ μm.[16] It extends laterally up to the vertical walls of the airbox, which provides an explicit electrical connection to ground. Because the focus is on the conductivity of the metal film, it is assumed to be non magnetic ($\mu_r = 1$) and the presence of its substrate is not accounted for (i.e. ϵ_r is set to 1 above the film).

The simulations are carried out using COMSOL multiphysics (version 4.0a, RF module) in the mode 2D/Electromagnetic Wave/Mode Analysis. They consist in solving the Maxwell equations describing the propagation of electromagnetic waves along an infinite transmission line having a cross-section as sketched on Fig. 1(a). The microwave frequency is fixed at $f = 2$GHz and the eigenvalue problem obtained after meshing the cross section into about 2000 triangles is solved, thus providing the allowed propagation mode and its propagation wave-vector k_z. As expected for the chosen design, one obtains only one propagation mode which is predominantly TEM ($E_z, \simeq 0,\ H_z \simeq 0$). From the simulation, the transverse distributions of the electric $[\mathbf{E}(x, y)]$ and magnetic $[\mathbf{H}(x, y)]$ fields are extracted together with the propagation index $n_{eff} = c2\pi k_z/f$ and the characteristic impedance $Z_c = V/I$ with $V = \int_P E_y.dy$ and $I = \oint_C \mathbf{H}.\mathbf{dl}$ [see the integration paths P and C in green in fig. 1(a)].

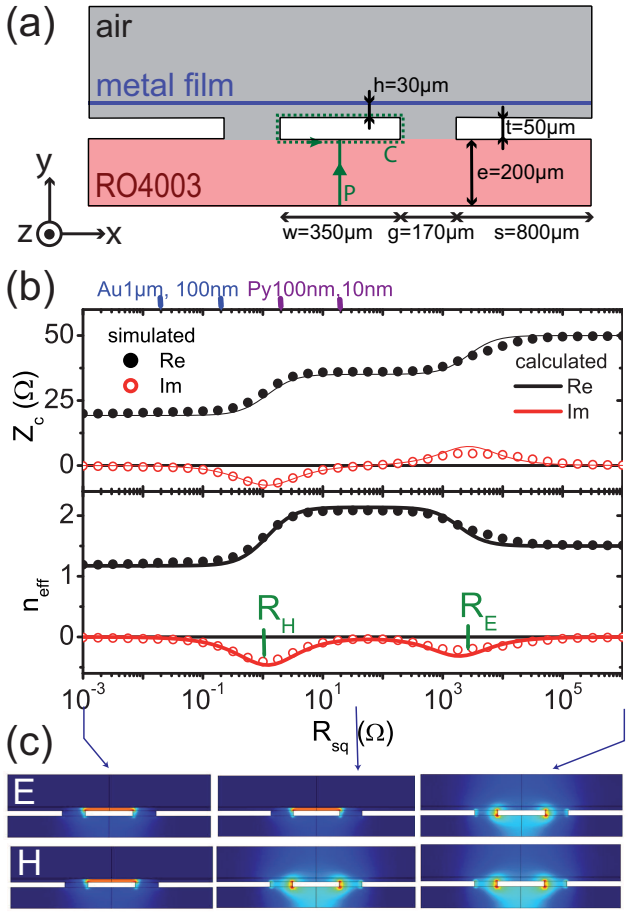

FIG. 1: (a) Geometry of the finite element simulation. (b) Results of the simulation of the propagation at a frequency of 2GHz (dots). The real and imaginary parts of the characteristic impedance Z_c (top) and the effective propagation index n_{eff} (bottom) are shown as a function of the resistance per square of the film R_{sq}. The lines are the results of the model of Fig.2. (c) Amplitude maps of the microwave electric field **E** and magnetic field **H** for R_{sq}=1 mΩ, 56 Ω and 1 MΩ (from left to right). Color scale: blue (zero) to red (maximum amplitude).

Note that n_{eff} and Z_c, which would be purely real if only perfect metals were involved, are expected to have non-zero imaginary parts due to the finite conductivity of the metal film. Figure 1(b) shows the real and imaginary parts of n_{eff} and Z_c as a function of the resistance per square of the film R_{sq}, varied between 10^{-3} and 10^6 Ω. One distinguishes clearly three plateaus for the real parts of n_{eff} and Z_c. These plateaus are separated by transition regions in which the real parts of n_{eff} and Z_c varies smoothly while their imaginary parts show peaks. Interestingly, different distributions of **E** and **H** are observed for each of

the three plateaus. This is illustrated in Fig. 1(c) which shows color plots of the amplitude of **E** and **H** for three selected values of the film resistance. For the highest values of R_{sq} (i.e. no conductance effect), one recovers the value $Z_c^{CPW} = 50\ \Omega$ and $n_{eff}^{CPW} = 1.5$ targeted in the design of the CCPW. Both **E** and **H** appear to be concentrated in the gaps between the center track and the lateral ground planes (Fig. 1c right).[17] On the other hand, for the lowest values of R_{sq} (i.e. a strongly conducting film), Z_c and n_{eff} are reduced to 20 Ω and 1.2 respectively, and **E** and **H** appear to be strongly concentrated in the air gap separating the center track and the metal film [Fig. 1(c) left]. For intermediate values of film resistance, one observes an intermediate value of Z_c (35 Ω) and a higher value of n_{eff} (2.1). Interestingly, the distributions of the electric and magnetic fields are different from each other: **E** is concentrated above the central track, as in the low resistance regime, while **H** is distributed around the central track, as in the high resistance regime [Fig. 1(c) middle]. These results are interpreted as follows: in the high resistance regime, the effect of the metal film is negligible and one recovers the characteristics of the unperturbed CCPW [see Fig. 2(a)]. In the low resistance limit, the metal film acts as a perfect ground plane which dominates over the other ground planes because of its proximity to the signal track. The propagation mode is then very close to that of a transmission line consisting of two parallel plates with air in between [PP, see Fig. 2(b)]. The propagation parameters of this transmission line are easily evaluated as $n_{eff}^{PP} \simeq 1$ and $Z_c^{PP} \simeq \sqrt{\mu_0\epsilon_0}h/w = 32\ \Omega$.[12] In this regime, the metal film acts as a perfect shield, i.e. it carries currents and charges opposite to those existing in the signal track so that the microwave field above the film is zero. Apparently a film of intermediate resistance allows for the shielding of the electric field but not for that of the magnetic field. This very special regime will be discussed later in the paper in terms of the so-called slow-wave effect.

Let us now model the observed behavior within the standard formalism of transmission lines. For a short length δ of the CCPW loaded with the metal film, the CPW propagation mode is modeled by combining a series inductance $L_{CPW}\delta$ and a parallel capacitance $C_{CPW}\delta$. To account for the competition with the PP mode, these are put in parallel with the inductance and capacitance of the PP mode [see Fig. 2(d)]. Series resistor are included in these two additional branches to account for the electrical resistance opposed by the metal film to the shielding currents: To confine the magnetic field below the metal film, a current j_H extending approximately over the width w should flow along the film in the direction

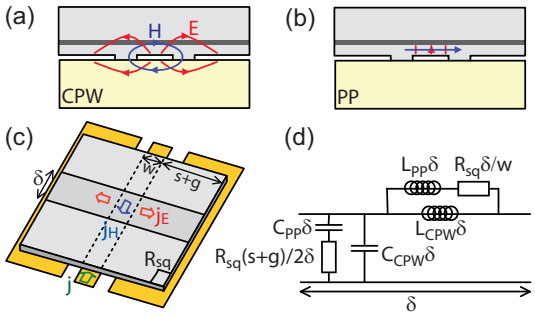

FIG. 2: (a,b) Sketches of the CPW and PP modes. (c) Sketch of the current j_H (resp. j_E) which has to flow along the metal film to shield the magnetic field (resp. the electric field). (d) Distributed impedance model accounting for the competition between the CPW and PP modes.

opposite to that of the central track current j [see Fig. 2(c)]. This translates into a resistance $R_{sq}\delta/w$ adding to the inductive parallel-plate branch. In a similar way, the shielding of the electric field requires currents j_E returning towards both lateral walls, which translates into a resistance $R_{sq}(s+g)/2\delta$ adding to the parallel branch. The lines in Fig. 1(b) show the global characteristic impedance and effective index deduced from the model of Fig. 2(d).[18] They reproduce extremely well the result of the simulation, which suggests that despite its simplicity the proposed model captures the physics of the observed phenomenon of microwave shielding.

For further simplification, it is possible to write in a compact way the maximum film resistance R_E (resp. R_H) allowing for the shielding of the electric (resp. magnetic) field. Assuming $C_{PP} \gg C_{CPW}$ and $L_{PP} \ll L_{CPW}$, one obtains $R_E = Z_c^{CPW}\lambda/\pi(s+g)$ and $R_H = Z_c^{CPW}w/2\pi\lambda$, where λ is the CPW propagation wavelength. Thus, the relevant shielding regime can be determined from a simple ratio of dimensions. Fig. 3 shows a phase diagram of the phenomenon of shielding. The transition film resistance R_E and R_H are plotted as a function of the frequency for three different sets of dimensions $(w, s+g)$ representative of the transmission lines used for broadband FMR. The first set, corresponds to the design investigated in this paper, typical of ultra-broadband transmission lines on printed circuit boards. The second set corresponds to a relatively narrow coplanar waveguide on a silicon or alumina substrate, typical of CPWs fabricated using thin film lithography techniques.[2,3] The third set corresponds to a relatively wide microstrip.[6] The typical values of film resistance and microwave frequencies used in CPW-FMR are shown as a gray rectangle. The phenomenon

of shielding appear to play an important role in most CPW-FMR experiments: the electrical field is expected to be completely shielded in nearly all cases, while the magnetic field is expected to be shielded in the thick film, high frequency, wide-CPW sector of the parameter space. Once again, we emphasize that this phenomenon of microwave shielding occurs for film thickness much smaller than the relevant skin depth. It actually appears as soon as the film resistance is small enough to allow for shunting currents to flow in it. It is therefore expected not to depend strongly on the simplifying assumptions of the model of Fig.1 (film substrate of dielectric constant unity, metal box, film explicitly connected to the ground). Once shielded, the electric and magnetic fields are indeed concentrated in the air gap separating the CPW and the film, so the properties of the film substrate are not of major importance. Moreover, even in the absence of an explicit ground connection of the film (films can be electrically floating in CPW-FMR experiments), the large capacitive coupling between the CPW ground planes and the film is expected to provide the required low impedance paths. Finally, let us comment on the dependence of the effect on the film height h. In Fig. 1(a), we have chosen a relatively high value of 30 μm because this facilitates the finite element simulations and the visualization of the modes. In most CPW-FMR experiments the film is placed directly above the film and its height is probably only limited by the relative planarities of the film and CPW top surface. The distance between the top of the center track and the film is therefore not expected to exceed a few micrometers (enough to avoid a direct short circuit). The main difference is that Z_c^{PP} -which scales as h/w- can now be very low, resulting in a more pronounced impedance mismatch in the shielding regime.

The phenomenon of shielding is expected to have two important consequences in a broad-band FMR experiment. (i) If the magnetic field is shielded, it is expected to decrease to zero across the film thickness.[9] Due to this strong inhomogeneity, perpendicular standing spin wave modes can be excited, in contrast with the unshielded case.[6,10] (ii) The shielding of **H** and/or **E** results in a strong modification of Z_c and n_{eff}. This is expected to change significantly the reflection and transmission coefficients of the loaded portion of the CPW (large impedance mismatch in the full shielding regime, increased transmission delay in the electric-only shielding regime, increased loss at the transitions between the three regimes). For a quantitative data analysis, these modified propagation characteristics should be accounted for in the de-embedding process.[3] Finally, let us briefly comment on the intermediate regime

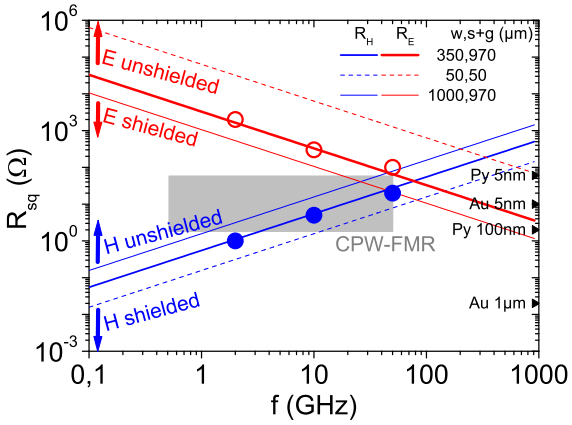

FIG. 3: Phase diagram for the phenomenon of microwave shielding. The threshold values R_E (red line) and R_H (blue line) are plotted as a function of the microwave frequency for three geometries of transmission lines (see details in the text). The dots show the values obtained from the simulation of Fig.1 at 2, 10 and 50 GHz. Typical square resistance for ferromagnetic metal films (Py) and non-magnetic films (Au) are shown on the right.

where only the electric field is shielded. Due to the fact that the spatial distributions of the electrical and magnetic field are completely decoupled in this regime, it is possible to tune the capacitance and inductance per unit length independently from each other by changing some dimensions in the structure. In particular, this allows one to design 50 Ω transmission lines with a very large value of n_{eff} (i.e. a very low wave velocity), which is known in the microwave community as a slow-wave effect.[13] This is used for integrated microwave circuits, in particular for reducing the footprint of delay lines and for reducing substrate losses in interconnects on non-insulating substrates (e.g. silicon).[13] The model described here allows one to understand very simply the architectures used to obtain slow-waves: semiconducting layer located below the CPW with a suitable doping (such that its square resistivity falls in the $R_E < R_{sq} < R_H$ range),[14] or array of metal strips oriented perpendicular to the CPW axis [such as j_E currents are allowed whereas j_H currents are forbidden, see Fig. 2(c)].[15]

To conclude, this paper provides an analysis of the propagation of electromagnetic waves along a coplanar waveguide over which a conducting film is placed. A full wave 2D electromagnetic simulation in a well controlled channelized coplanar waveguide geometry shows that such a film is able to shield completely the electric and/or the magnetic field of the CPW depending on the value of its square resistance. These results are interpreted quanti-

tatively with the help of a simple distributed impedance model accounting for the shielding currents likely to flow along the metal film. This model allows one to predict the range of parameters for which shielding of the electric and/or magnetic fields is expected to occur. From this it is concluded that the phenomenon should be accounted for in the analysis of most broadband inductive measurements of ferromagnetic resonance performed on metal ferromagnetic films.

The author would like to thank O. Bengone and C. Tugene (IPCMS) for their assistance with the simulations, B. Rosas and D. Leavitt (Southwest Microwave) and C. Candun (Elexo) for providing test boards and J. Will (IUT Louis Pasteur) for preliminary measurements and Y. Henry (IPCMS) for useful discussions. This work was supported by the ANR (NanoSWITI, ANR-11-BS10-003).

---

* Electronic address: bailleul@ipcms.unistra.fr

[1] Y. Ding, T. J. Klemmer, and T. M. Crawford, Journal of Applied Physics **96**, 2969 (2004).

[2] J.-M. Beaujour, W. Chen, K. Krycka, C.-C. Kao, J. Z. Sun, and A. D. Kent, The European Physical Journal B **59**, 475 (2007), ISSN 1434-6028.

[3] C. Bilzer, T. Devolder, P. Crozat, C. Chappert, S. Cardoso, and P. P. Freitas, Journal of Applied Physics **101**, 074505 (pages 5) (2007).

[4] S. S. Kalarickal, P. Krivosik, M. Wu, C. E. Patton, M. L. Schneider, P. Kabos, T. J. Silva, and J. P. Nibarger, Journal of Applied Physics **99**, 093909 (pages 7) (2006).

[5] T. Devolder, P.-H. Ducrot, J.-P. Adam, I. Barisic, N. Vernier, J.-V. Kim, B. Ockert, and D. Ravelosona, Applied Physics Letters **102**, 022407 (pages 4) (2013).

[6] K. J. Kennewell, M. Kostylev, N. Ross, R. Magaraggia, R. L. Stamps, M. Ali, A. A. Stashkevich, D. Greig, and B. J. Hickey, Journal of Applied Physics **108**, 073917 (pages 12) (2010).

[7] T. J. Silva, C. S. Lee, T. W. Crawford, and C. T. Rogers, J. Appl. Phys. **85**, 7849 (1999).

[8] G. Counil, J.-V. Kim, T. Devolder, C. Chappert, K. Shigeto, and Y. Otani, Journal of Applied Physics **95**.

[9] M. Kostylev, Journal of Applied Physics **106**, 043903 (pages 14) (2009).

[10] M. Kostylev, A. A. Stashkevich, A. O. Adeyeye, C. Shakespeare, N. Kostylev, N. Ross, K. Kennewell, R. Magaraggia, Y. Roussigne, and R. L. Stamps, Journal of Applied Physics **108**, 103914

(pages 8) (2010).

[11] B. Rosas, Tech. Rep., Southwest Microwave, Inc. (2011), available at `http://mpd.southwestmicrowave.com/resources/`.

[12] S. Ramo, J. R. Whinnery, and T. van Duzer, *Fields and Waves in Communication Electronics* (Wiley, 1984), 2nd ed.

[13] T. Cheung and J. Long, Solid-State Circuits, IEEE Journal of **41**, 1183 (2006).

[14] H. Hasegawa and H. Okizaki, Electronics Letters **13**, 663 (1977).

[15] S. Seki and H. Hasegawa, Electronics Letters **17**, 940 (1981).

[16] In order to limit the number of mesh elements, the metal film is modeled as a relatively thick layer ($t_{film} = 10$ μm) with a conductivity $\sigma = (R_{sq} t_{film})^{-1}$. It was checked that the result of the simulation does not change when t_{film} is decreased to more realistic values while R_{sq} is fixed.

[17] High values of E and H are also observed in the substrate immediately below the center track. This is is typical for a CCPW with a relatively thin substrate which represents a situation intermediate between a conventional CPW and a microstrip.

[18] We use $Z = Z_c n\omega/c$ and $Y = n\omega/(cZ_c)$ to relate the series impedance Z and parallel admittance Y per unit length to Z_c and n_{eff} for the CPW and PP modes and for their combination.[12]